sustainability

MDPI

Article

Eco-Friendly Reinforced Concrete Beams Exposed to Standardized Fire: A Thermal Finite Element Analysis

Fabricio L. Bolina * and Arthur S. Henn

Structures and Civil Construction Department (DECC), Civil Engineering, Federal University of Santa Maria (UFSM), Santa Maria 97105-900, Brazil; arthur.henn@acad.ufsm.br
* Correspondence: fabricio.bolina@ufsm.br

Abstract: Concrete has a significant impact on the environment and efforts are being made to replace it with more environmentally friendly alternatives. One possibility is to replace all or part of the conventional components (i.e., cement, water, sand and gravel) with recyclable solutions. Several studies have already demonstrated the mechanical and ecological suitability of the new eco-concretes, but the safety of structures built with them is not considered in the literature, which indicates a lack of knowledge. The purpose of this study is to evaluate the fire safety of reinforced concrete beams built with eco-friendly concretes and compare them to conventional concretes. The analysis was performed numerically and solved with Abaqus software using the finite element method, assuming the thermal parameters previously proposed in the literature through experimental investigations. The thermal field generated in beams with eco-concrete is a maximum of 50% lower compared to conventional concrete and the temperatures of the reinforcement are reduced by a maximum of 260%. There is an interesting perspective for the use of these materials in terms of fire safety criteria.

Keywords: reinforced concrete; beams; finite element; fire safety; sustainability

check for updates

Academic Editor: Francesco Asdrubali

Received: 19 February 2025
Revised: 7 March 2025
Accepted: 20 March 2025
Published: 26 March 2025

Citation: Bolina, F.L.; Henn, A.S. Eco-Friendly Reinforced Concrete Beams Exposed to Standardized Fire: A Thermal Finite Element Analysis. *Sustainability* **2025**, *17*, 2951. https://doi.org/10.3390/su17072951

Copyright: © 2025 by the authors. Licensee MDPI, Basel, Switzerland. This article is an open access article distributed under the terms and conditions of the Creative Commons Attribution (CC BY) license (https://creativecommons.org/licenses/by/4.0/).

1. Introduction

With the increasing levels of environmental pollution and carbon footprints, the use of sustainable materials in building construction has become a subject of extensive discussion. The United Nations Conference on Environment and Development (UNCED), commonly known as the Rio-92 Earth Summit, held in Rio de Janeiro in 1992, was a pivotal event in the discourse on global sustainability. One of its cornerstone documents, Agenda 21, emphasized the necessity of reducing industrial emissions, including those from the cement industry, as part of global efforts to mitigate climate change and promote sustainable development.

According to Andrew (2018) [1], the cement industry is one of the largest contributors to CO_2 emissions in the industrial sector, accounting for approximately 7–8% of global greenhouse gas emissions. This is predominantly due to the calcination process, where limestone ($CaCO_3$) is heated to produce clinker, releasing substantial amounts of carbon dioxide. Furthermore, the reliance on fossil fuels in cement kilns exacerbates these emissions.

In this context, sustainable concretes emerge as a potential solution to reduce atmospheric CO_2 emissions, as they typically contain reduced cement content while maintaining comparable performance parameters. However, a significant gap in literature lies in the limited studies on the performance of sustainable concretes under varying temperature conditions. Although the use of admixtures and recycled materials in concrete has gained

prominence, there is little research on their behavior at high temperatures, making it difficult to understand their durability and performance in fire incidents, raising concerns about their safety and applicability in critical scenarios.

In El Boukhari et al. (2023) [2], the use of Olive Pomace (OP) and Olive Mill Waste Water (OW) to produce two types of fine aggregates, namely Olive Pomace (OP) and Olive Pomace immersed in Olive Mill Waste Water (OPW), was explored. These materials are by-products of olive farming, and their improper disposal can harm the environment by contaminating groundwater and rivers. The study observed that substituting natural sand with OW led to reductions in both compressive strength and thermal conductivity.

El-Aidy et al. (2024) [3] investigated the use of Recycled Plastics (RP) as substitutes for fine and coarse aggregates. Plastics are produced on a large scale and require proper disposal methods, such as recycling, landfilling, or incineration. However, incineration contributes to air pollution, and landfilling demands extensive space while posing risks of clogging drainage systems. The study found that complete replacement of fine aggregates with recycled plastic caused greater reductions in mechanical strength compared to the complete replacement of coarse aggregates. Nevertheless, higher plastic content decreased thermal conductivity and density, thereby reducing self-weight.

Aghamohammadi et al. (2024) [4] evaluated the use of slag and calcium oxide (CaO) as cement substitutes, along with rubber powder and PET as replacements for fine aggregates. Rubber does not decompose naturally and causes environmental issues, while burning it releases toxic gases, and landfilling leads to soil contamination. PET, extensively used globally, generates significant waste that is often ingested by wildlife in various ecosystems. According to Tamburini et al. (2025) [5], approximately 34 billion PET bottles have ended up in marine environments. The incorporation of these materials into concrete helps address waste management challenges while promoting sustainability.

Mydin et al. (2023) [6] analyzed the use of burned rice husk and palm oil carbonate as substitutes for cement. Rice Husk Ash (RHA) and Palm Oil Fuel Ash (POFA) are by-products of rice and palm oil processing industries. If not disposed of properly, these materials can cause significant environmental damage, including soil and water contamination. Their use in concrete production mitigates these issues and reduces greenhouse gas emissions from agricultural and industrial waste.

Ahmed et al. (2022) [7] studied the use of Waste Polypropylene (WPP) as a fine aggregate substitute. WPP, widely utilized in packaging and plastic products, poses significant environmental challenges due to its slow degradation. This contributes to increased solid waste in landfills and pollution in terrestrial and aquatic ecosystems. Its persistence in the environment harms wildlife, which often ingests plastic particles, releasing microplastics into the food chain. The incineration of polypropylene as a disposal method releases toxic gases and exacerbates climate change.

Conifer Pine Ash (CA) and Conifer Leaf Ash (LA), as described by Gharibi et al. (2023) [8], are renewable resources with potential as natural alternative materials. In the context of rising energy consumption, their use is suggested as a sustainable solution to enhance energy efficiency, highlighting the importance of leveraging renewable resources for sustainable development. By utilizing CA and LA, these materials offer an eco-friendly alternative to traditional cement, reducing environmental impact and promoting innovative, sustainable construction practices.

As highlighted by Xu et al. (2024) [9], the extraction of conventional aggregates requires substantial energy and causes significant environmental degradation. In their study, waste wood and foam were used as alternatives to traditional aggregates, offering a sustainable solution that reduces the exploitation of natural resources and minimizes environmental impacts. Waste wood, a frequently discarded and underutilized by-product, was employed

as a filler to replace natural fine aggregates, while foam was introduced to create a cellular porous structure within the concrete. This combination not only reduces the bulk weight and thermal conductivity of the concrete but also enhances its thermal insulation, low-temperature resistance, and corrosion resistance properties. By utilizing waste wood and foam in place of conventional aggregates, the study demonstrates a promising approach to more sustainable and environmentally friendly construction practices.

Paiva et al. (2024) [10] addressed the use of bio-aggregates, specifically bamboo particles, wood shavings, and rice husk ash, as substitutes for coarse aggregate. With the rise in toxic gas emissions, there is a growing demand for sustainable materials that exhibit thermal and mechanical performance suitable for building applications. Bio-aggregates, being abundant agricultural residues, are easily accessible and help reduce landfill waste. The study noted that incorporating bio-aggregates reduces thermal conductivity; however, it did not address their mechanical performance, such as compressive strength.

In this research, different sustainable concretes (i.e., eco-friendly concretes) were analyzed, focusing on their thermal and physical properties. A total of 20 concrete beams are modeled using the finite element method and solved using Abaqus software version 2016, with each beam corresponding to a specific mix design (i.e., eco-friendly concrete case). The beams are then evaluated to determine their thermal behavior and safety in fire scenarios.

2. Materials and Methods

The paper aims to analyze (through numerical analysis) the temperature distribution in beams cross-sections exposed to fire, assuming the thermal and physical parameters of eco-concrete proposed in the literature (described in Section 2.5) by experimental procedures. The results of the temperatures in the cross-section were compared with conventional concretes when the thermal and physical parameters are standardized.

The materials and methods are shown below.

2.1. General Description of the Research

The purpose of this article is to provide a literature review on eco-friendly concretes, in particular on those researches that aim to define the thermal and physical properties of these materials. Eco-friendly concretes were considered to be those that propose a partial or total replacement of the cement or aggregates with recycled materials in order to improve the sustainability of conventional concrete and reduce the associated environmental damage. In order to understand the fire behavior of buildings with eco-friendly concrete, a series of finite element modeling of beams was performed assuming the thermal and physical data proposed in the literature. The research aimed to understand the safety of beams built with eco-friendly concrete and the viability of replacing conventional concrete with green concrete in terms of building safety in fire situations.

2.2. Eco-Friendly Concrete Cases

Table 1 shows the nomenclature and properties of the concrete mixtures considered in this study. The specimens and concrete mixes contain different proportions of materials such as olive pomace, recycled plastic, rubber, PET, rice husk ash, palm oil fuel ash, polypropylene waste, conifer pine, leaf ash, wood, foam, bamboo and bio-based components. These variants aim to explore the impact of green materials by partially or completely replacing traditional components in conventional concrete, such as cement, water, sand or gravel. The mixes of each concrete presented are defined in Appendix A.

Table 1. Concrete cases assumed and nomenclatures.

Nomenclature (Concrete Case)	Description
C1-OP	10% Olive Pomace Concrete
C2-OPw	10% Olive Pomace immersed in Olive Mill Waste Water Concrete
C3-RPs	Recycled Plastic Concrete 100% sand replacement
C4-RPg	Recycled Plastic Concrete 50% gravel replacement
C5-Ru	10% Rubber Concrete
C6-Pet	10% PET Concrete
C7-RH10	10% Rice Husk Ash Concrete
C8-RH40	40% Rice Husk Ash Concrete
C9-PO10	10% Palm Oil Concrete
C10-PO40	40% Palm Oil Concrete
C11-WP8	8% Waste polypropylene Concrete
C12-WP40	40% Waste polypropylene Concrete
C13-CA	10% Conifer Pine Ash Concrete
C14-LA	10% Conifer Leave Ash Concrete
C15-WFC1	40% Wood 1% Foam Concrete
C16-WFC2	40% Wood 2% Foam Concrete
C17-WFC3	40% Wood 3% Foam Concrete
C18-BBC	40% Bamboo Bio Concrete
C19-WBC	40% Wood Bio Concrete
C20-RHBC	40% Rice Husk Ash Bio Concrete

C1-OP incorporates 10% Olive Pomace (OP) and C2-OPw includes 10% Olive Pomace immersed in Olive Mill Waste Water (OPW) as partial substitutes for fine aggregates. C3-RPs substitutes 100% of fine aggregates (sand) with Recycled Plastic (RP), while C4-RPg replaces 50% of coarse aggregates (gravel) with RP. C5-Ru and C6_Pet substitute a total of 10% of fine aggregates with Rubber and PET, respectively. C5 and C6 mixes use slag as a replacement for cement. C7-RH10 and C8-RH40 incorporating 10% and 40% Rice Husk Ash (RHA) as partial cement replacements, respectively. Similarly, C9-PO10 and C10-PO40 uses, respectively, Palm Oil Fuel Ash (POFA) at substitution rates of 10% and 40%. C11-WP8 and C12-WP40 replacing fine aggregates with Waste Polypropylene (WP) at 8% and 40%, respectively. C12-CA and C14-LA substitute 10% of cement with Conifer Pine Ash (CA) and Conifer Leaf Ash (LA), respectively. C15-WFC1, C16-WFC2 and C17-WFC3 replacing 40% of natural fine aggregates with Waste Wood, and incorporating 1%, 2%, and 3% foam, respectively, to create a cellular porous structure. Additionally, C18-BBC replaces 40% of coarse aggregates with bamboo particles, while C19-WBC substitutes 40% with wood shavings, and C20-RHBC uses 40% Rice Husk Ash (RHA) as a replacement for coarse aggregates.

The criteria for the selection of research papers in the literature are the use of eco-friendly concretes (i.e., concretes with a certain amount of recycled material in the mix, e.g., to reduce cement consumption).

2.3. Thermo-Physical Parameters

The thermal properties of the individual concretes considered in Table 1 are listed in Table 2. In this paper, only the research that has already defined the thermal parameters

of green concrete has been used. The reference is already given. Thermal conductivity and density are parameters that help to understand the level of heating of structures exposed to fire, as described in Section 2.5. If the authors did not define the density in their study, the value proposed in EN 1992-1.1 [11] was taken into account (i.e., 2400 kg/m^3). The conventional concrete assumed as a reference has a constant thermal conductivity of 1.8 W/m°C and a density of 2400 kg/m^3. In all cases, the specific heat was assumed to be 900 J/kg°C.

Table 2. Thermo-physical parameters assumed to the eco-friendly concretes.

Nomenclature	Thermal Conductivity (W/m°C)	Density (kg/m^3)	Reference
C1-OP	0.6	2013.5	El Boukhari et al. [2]
C2-OPw	0.6	2095.8	
C3-RPs	1.1	1913.0	El-Aidy et al. [3]
C4-RPg	1.25	2037.0	
C5-Ru	1.03	2301.5	Aghamohammadi et al. [4]
C6-Pet	1.16	2426.7	
C7-RH10	0.38	1185.0	Mydin et al. [6]
C8-RH40	0.38	1167.0	
C9-PO10	0.365	1177.0	
C10-PO40	0.33	1158.0	
C11-WP8	1.35	2350.0	Ahmed et al. [7]
C12-WP40	0.75	2150.0	
C13-CA	1.35	-	Gharibi et al. (2023) [8]
C14-LA	1.33	-	
C15-WFC1	0.34	1466.0	Xu et al. [9]
C16-WFC2	0.27	1420.1	
C17-WFC3	0.26	1379.5	
C18-BBC	0.25	1214.9	Paiva et al. [10]
C19-WBC	0.24	1211.4	
C20-RHBC	0.25	1204.0	

2.4. Beams Cross-Section Cases

Two beam cross-sections were considered in the analysis (B1 and B2, as shown in Table 3). The cross-section width (W) and height (H) of both beams are shown in Table 3 and Figure 1. The thickness of the slab (ts) was set at 120 mm. The cross-section shown in Figure 1a contains the control points assumed to determine the average temperature of steel and concrete for the design of the sagging bending resistant moment (+) of the RC beams (the concrete temperature above the neutral axis and the positive steel reinforcements as used in the conventional structural design procedure). The same in Figure 1b, but for the hogging moment (−).

The temperature time history of concrete (average between control points pt1 to pt5) and reinforcement temperatures (average between control points Rb1 to Rb3) was monitored to determine the thermal field of each selected cross-section (Table 3). Since the concrete cross-section at the bearing capacity of the beam is above (in case of sagging moment) or below (hogging moment) the neutral axis, only measurement points in this region were assumed for the concrete temperatures (i.e., 0.5 × H). The concrete temperature

is the average of the control points pt1(+) to pt5(+) (in the case of the sagging moment) and pt1(−) to pt5(−) (hogging moment).

Table 3. Beams cross-section assumed.

Cross-Section Characteristics and Nomenclatures				
Beam Number	**Nomenclature**	**Width W (mm)**	**Height H (mm)**	**C_f Thickness (mm)**
1	B1	200	500	20 to 50
2	B2	300	500	20 to 50

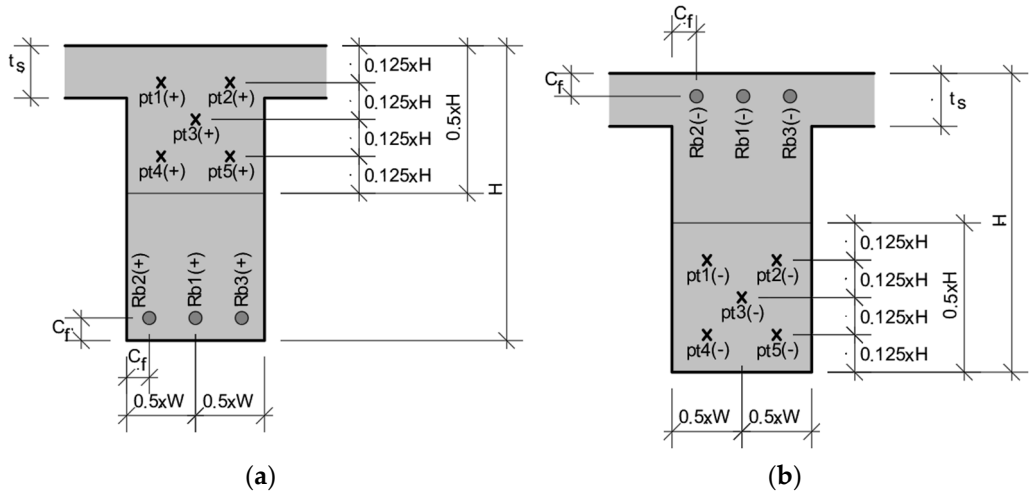


Figure 1. Cross-section set-up: control points considered in the (**a**) sagging and (**b**) hogging bending moment in the beams cross-section.

2.5. Finite Element Modeling

This study is based on a thermal analysis that was solved with the software Abaqus [12]. Equation (1) shows the governing equations used to define the temperature field and transfer in the cross-sections assumed in the analysis. The thermal diffusivity is related to the mass loss, the thermal conductivity λ and the specific heat C_p. These parameters are those proposed in Table 2 for each assumed concrete case. Due to the lack of results in the literature, C_p was assumed as 900 J/kg.°K in all cases [13]. For the concrete assumed as reference, all parameters are those proposed in Eurocode [13]. In the case of reinforcement, the thermal parameters in the model are not necessary, since the temperature in the rebars was considered to be the same in the concrete in the same layer as the results proposed in similar full-scale experimental studies ([14,15]). In this sense, the characteristics of the reinforcement (cross-section, type of material, etc.) are not necessary. The arrangement of the rebars is shown in Figure 1a.

$$\alpha = \frac{\lambda}{\rho \cdot C_p} \quad (1)$$

Equation (2) defines the governing equation for convective and radiative heat transfer process [16], where n_y and n_z are the vector components of the outward perpendicular to the cross-sectional area; h_{rad} and h_{con} are the radiative and convective heat transfer coefficients, respectively; T is the ambient temperature (assumed as 20 °C) and T_E is the temperature of the environment subjected to fire (considered as ISO 834 [17] standardized time-temperature, as proposed by EN 1992-1.2 [13] to structural design in case of fire). The radiation heat transfer coefficient is given by Equation (3) (it was assumed for all cases, as there is no discussion about this coefficient for the eco concretes), where σ is

the Stefan-Boltzmann constant ($\sigma = 5.67 \times 10^{-8}$ W/m^2 °C^4), and ε the emissivity factor (assumed as 0.70 according to EN 1992-1.2 [12]). As shown in Figure 2, the convective heat transfer was 25 and 9 W/m^2 °C on the surface exposed to the fire and the unexposed surface respectively. Heating was applied to the bottom surface of the beam, as is common in residential buildings exposed to internal fires.

$$k \cdot \left(\frac{dT}{dy} \cdot n_y + \frac{dT}{dz} \cdot n_z \right) = -(h_{rad} + h_{con}) \cdot (T - T_E) \quad (2)$$

$$h_{rad} = 4 \cdot \sigma \cdot \varepsilon \cdot \left(T^2 + T_E^2 \right) \cdot (T + T_E) \quad (3)$$

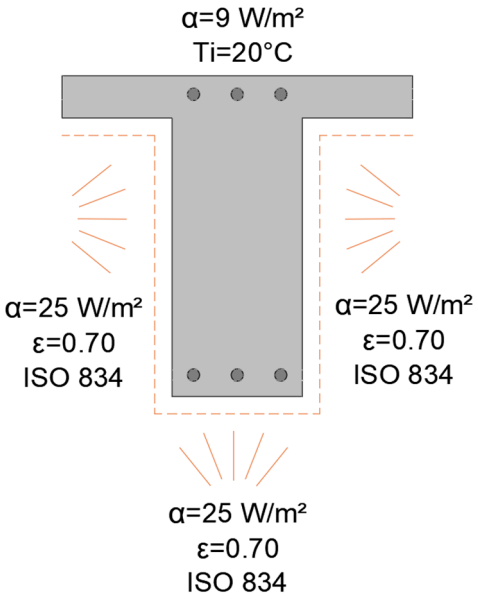


Figure 2. Heating process and parameters of the assumed beam cross-sections.

The problem is solved using a 3D model and a non-linear thermal transient analysis. The Abaqus library was used to represent the concrete as a finite element DC3D8 with classical integration. The mesh is quite fine-meshed with a size of 1.0 × 1.0 × 1.0 mm. A convergence criterion of 0.1 °C and a time increment of 0.001 s was used.

The criteria and procedure for the FE model (finite elements, mesh size, mesh validation, steps, boundary conditions, governing equations, etc.) were validated by the authors through an extensive full-scale experimental test. Some of these results and criteria can be found in [15,18,19]. The numerical simulation is also based on the approaches presented by the authors in [20], standards [21] and by others [22].

The following flowchart summarizes the finite element modeling: Create the cross section with solid DC3D8 finite elements, added the material thermal and physical parameters in the material properties, adopts the boundary conditions proposed in the Figure 2, meshing the model, create the control points (see Figure 1) to identify the temperature evolution in the cross section, set run and analyzed the results.

3. Results and Discussion

The results are presented in four parts: (i) concrete temperature, (ii) positive and (iii) negative reinforcement temperature, and (iv) cross-sectional temperature field.

3.1. Concrete Temperatures

The temperature profile in the concrete cross-section is shown in Figure 3. Figure 3a and Figure 3b show the average temperature between pt1(+) to pt5 (+) control points to

B1 and B2 beams, respectively. Figure 3c and Figure 3d show the same for the average temperatures from pt1(−) to pt5(−) for B1 and B2 respectively. The critical temperature of concretes (around 350 °C) stated in the literature was also emphasized. Appendix B shows the temperature in some standardized times.

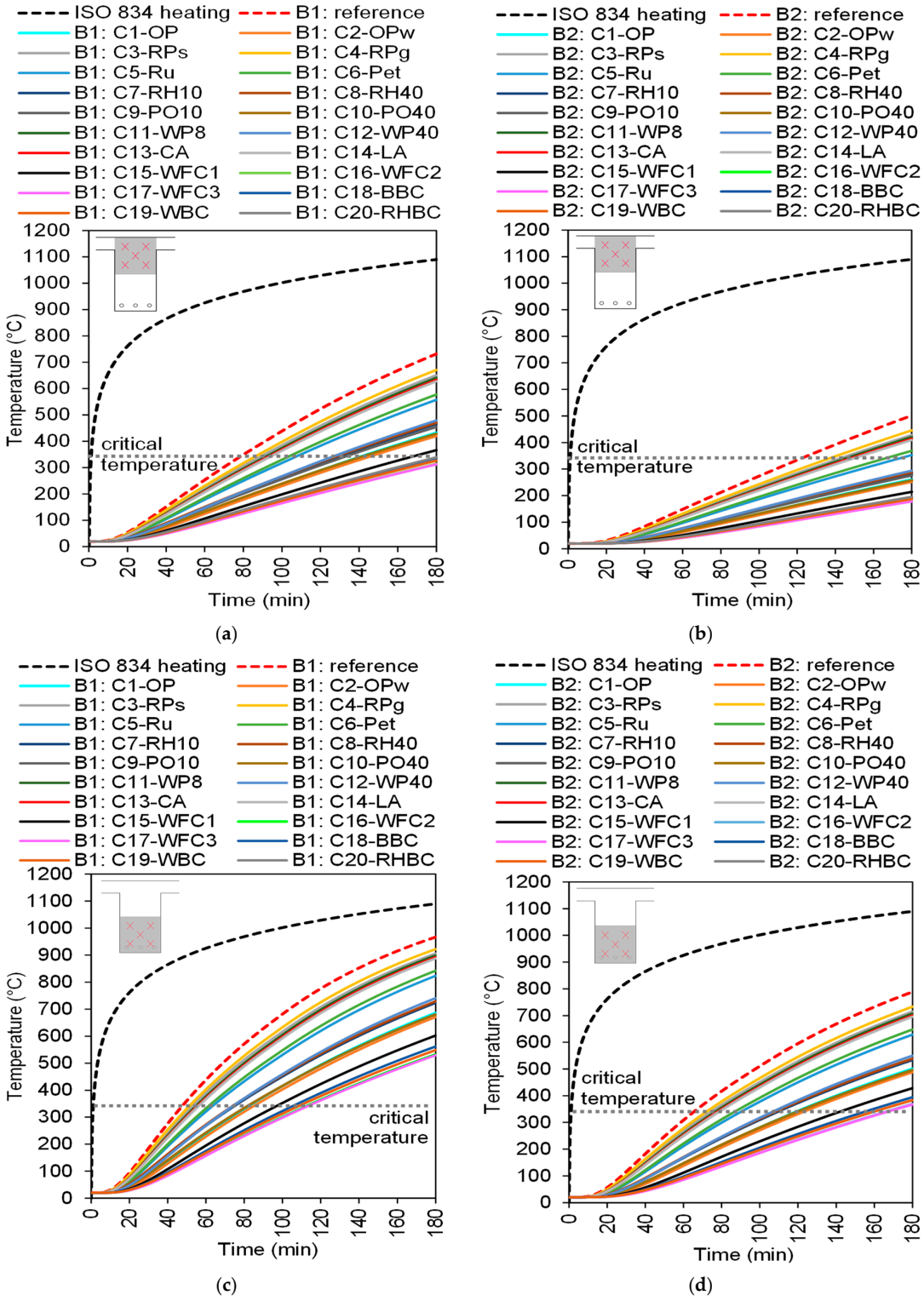


Figure 3. Temperature field in the concrete cross-section. (**a**) pt1(+) to pt5(+) control points on beam B1, (**b**) pt1(+) to pt5(+) control points on beam B2, (**c**) pt1(−) to pt5(−) control points on beam B1, (**d**) pt1(−) to pt5(−) control points on beam B2.

Figure 3 shows that all eco-friendly concretes tested exhibit lower heating compared to conventional concrete (i.e., the reference). The cross-sectional temperature field that develops in the tested eco-concretes is lower compared to the conventional solution. Based on the assumption that the temperature is lower, it can be expected that the mechanical damage caused by fire in these structures also tends to be lower compared to conventional concrete, suggesting good mechanical performance of the green structures in the event of fire.

The lower temperature field was observed in the beams built with concrete #17, i.e., the concrete mixes with 40% wood 3% foam (C17-WFC3). These concretes develop a temperature 350 °C (or around 50%) lower than conventional concrete at the end of the fire (i.e., after 180 min of fire exposure). This is probably due to the lower thermal conductivity of the wood and the air generated by the foam inclusion. Temperatures in C17 WFC3 concrete developed more slowly, suggesting that beams constructed with these materials developed very interesting mechanical performance in the event of a fire, withstanding heating for longer without collapsing in relation to conventional concrete (reference).

The green concrete (eco-friendly) with the worst fire behavior was C4-RPg, i.e., the concrete with recycled plastic in its composition. These concretes have a higher thermal diffusivity (see Equation (1) and Figure 3) compared to all other solutions proposed in the literature. Despite this characteristic, the temperature fields generated in the cross-section of the beams built with these concretes are lower than with the conventional concrete solution (i.e., reference concrete). At the end of the analysis, the temperature difference between conventional concrete and C4-RPg did not exceed 60 °C, indicating a very similar performance compared to the conventional solution (reference).

C7-RH10, C8-RH40 and C12 WP40 are concretes with a medium behavior compared to the two extremes mentioned above (C17 and C4). These concretes have mixtures with 10% (C7-RH10) and 40% rice husk ash (C8-RH40) and 40% polypropylene waste (C12 WP40). See the mixtures of these concretes in Appendix A. At the end of the fire test, these concretes had a temperature difference compared to the conventional concrete that did not exceed 250 °C, which highlights these residues as an intermediate solution to be incorporated into the concrete and also to reduce the temperature field in the cross-section of the structures in the event of a fire.

The cross-sectional dimensions of the structures are another aspect that changes the temperature field in the cross-section in parallel with the thermal and physical properties of the materials. This analysis becomes clear when comparing the results of B1 and B2 in Figure 3. However, it is not the aim of this research to perform a critical analysis of the influence of the geometries of the structures on the fire event.

3.2. Positive Reinforcements Temperatures

The temperature history of the positive reinforcements of the tested beams is shown in Figure 4. Figure 4a and Figure 4b show the average temperature between Rb1(+) to Rb3(+) in beam B1, assuming a concrete cover thickness (C) of 20 and 50 mm respectively. The same applies to beam B2 in Figure 4c and Figure 4d, respectively. Appendix B shows the temperature in some standardized ISO 834 [17] times.

The reinforcement is the most vulnerable part of reinforced concrete structures. Failure of the reinforcement leads to the collapse of the entire structure. In the literature, 500 °C [21] is usually given as the critical, which are highlighted in Figure 4. At this temperature, mechanical damage to the reinforcement is relevant and the structure is then susceptible to (local or global) failure due to the ultimate sagging bending moment capacity.

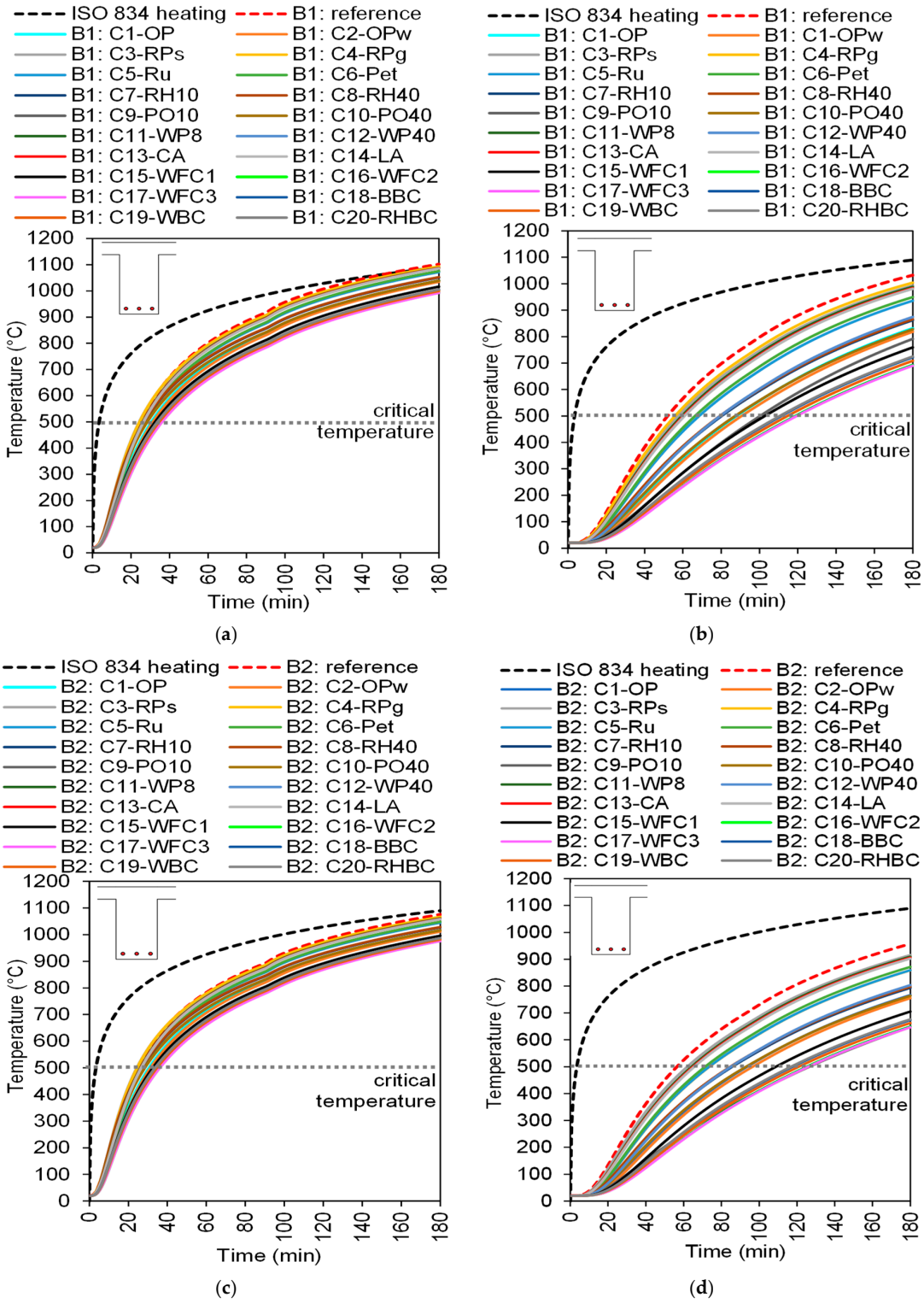


Figure 4. Temperature field in the positive reinforcements. (**a**) Rb1(+) to Rb3(+) control points on beam B1 (C = 20 mm), (**b**) Rb1(+) to Rb3(+) control points on beam B1 (C = 50 mm), (**c**) Rb1(+) to Rb3(+) control points on beam B2 (C = 20 mm), (**d**) Rb1(+) to Rb3(+) control points on beam B2 (C = 50 mm).

The thickness of the concrete cover has an inverse effect on the temperature development in the reinforcement. The greater the total thickness of the concrete, the lower the temperature in the reinforcement. In addition, the thermal and physical properties of the concrete can support and influence the temperature development in the reinforcements.

It is important to note that all reinforcements reach the critical temperature of 500 °C, regardless of the concrete cover thickness and concrete case. However, the critical temperature is reached at different times during the fire. The greater the concrete cover thickness, the clearer the differences between the concrete cases in the steel temperatures. This is due to the thickness of the concrete, which improves the influence of these variables (and then the thermal and physical parameters of the mixtures) on the results.

Assuming a concrete thickness of 20 mm, the difference between the mixtures is no more than 15 min. These differences are small and allow the conclusion that with a low concrete cover thickness, the influence of the concrete mix has no significant effect on the results. If the maximum concrete cover thickness is taken into account (i.e., C = 50 mm), the influences are more significant. In this case, the time for the reinforcement to reach its critical temperature can be improved in the order of 80 min, suggesting and fire resistance time improvement in order of 260%. These differences can be observed by comparing the C17-WFC3 with the reference concrete (made with conventional materials).

According to the previous analysis, C4-RPg shows a very similar fire behavior compared to conventional concrete. In this sense, this material does not improve the fire behavior of the beams, but represents a more environmentally friendly solution and can be competitive with conventional concrete when it comes to producing a thermally competent beam during a fire event. However, this information must also be analyzed from a mechanical point of view, i.e., to understand the total applied load on the beam built with this fire-damaged concrete.

As mentioned in the preceding analysis (i.e., Section 3.1), all eco-friendly concretes tested had a lower temperature history than conventional concrete. Based only on thermal considerations, the inclusion of residues in the concrete, in addition to reducing the environmental impact of this material on nature, can also minimize the temperature distribution in the cross-section and in the steel reinforcements, making this solution an appealing alternative to building green construction. The total time in which the critical temperature of the reinforcement is reached during a fire event is reduced, and probably the time in which the structure collapses during a fire can be improved.

The cross-section dimensions, which also have an influence on the temperature distribution in the reinforcements, are another variable that must be taken into account when designing structures in the event of fire. However, the cross-section geometries are not primarily considered in the discussion of this research.

3.3. Negative Reinforcements Temperatures

The temperature distribution in the negative reinforcements of the beams during the fire exposure is shown in Figure 5. Figure 5a and Figure 5b apply to beam B1 with 20 and 50 mm concrete cover respectively. Figure 5a,b apply to beam B2 with 20 and 50 mm concrete cover. The temperatures presented refers to the average between the Rb1(−) to Rb3(−) control points shown in Figure 1. Appendix B also shows the temperature in some standardized ISO 834 [17] times.

The negative reinforcements are more fire-resistant than the positive ones, so that the hogging bending moment of these beams is more stable than the sagging bending moment in the event of fire.

Is important to note that in all tested cases of environmentally friendly beams, the critical temperature of the reinforcement is not reached. However, with a concrete cover thickness of C = 50 mm, the beam produced with the reference concrete (i.e., conventional materials) reaches 500 °C, which leads to mechanical damage of the hogging bending moment in B1, which has the smaller cross-sectional dimensions.

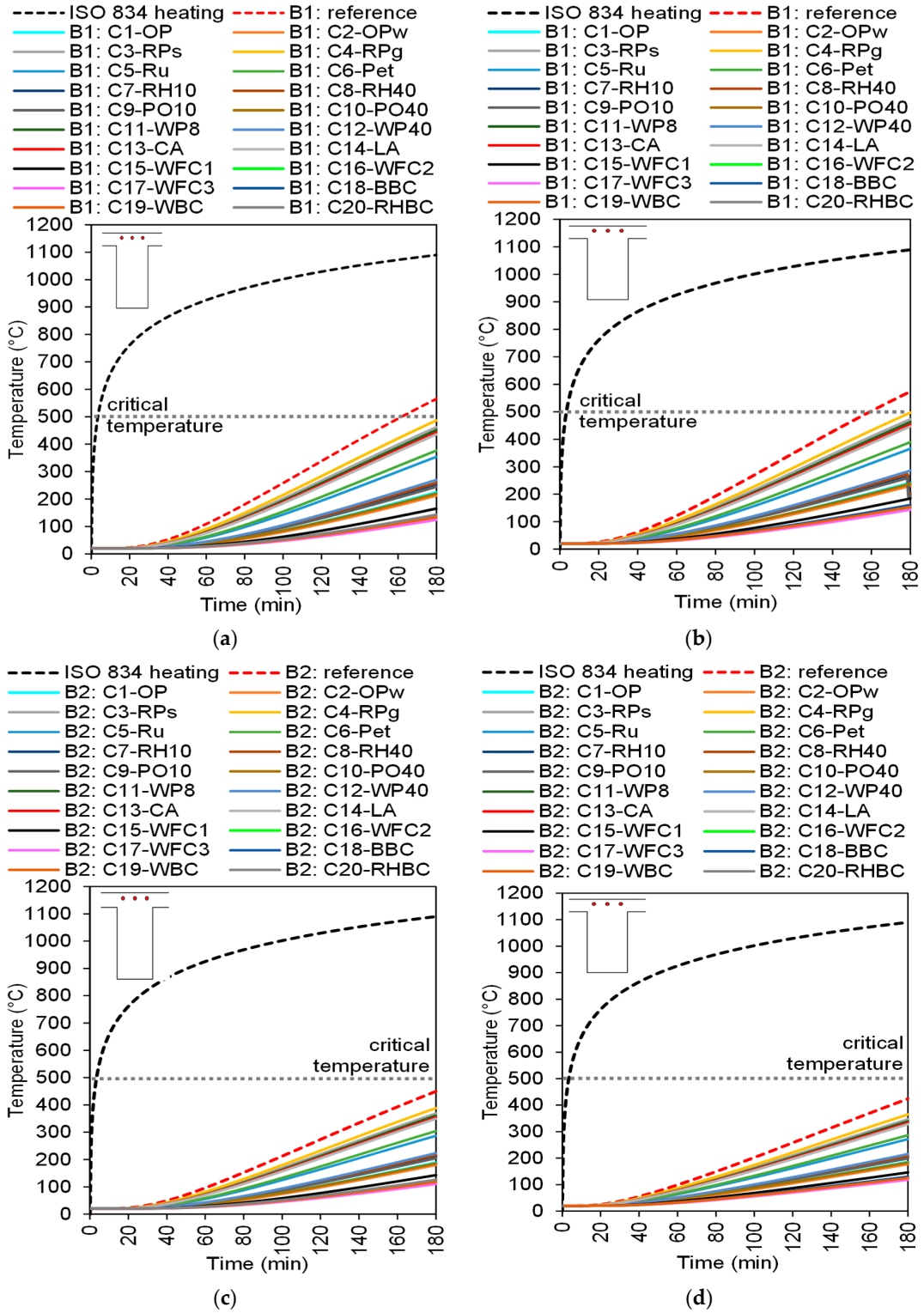


Figure 5. Temperature field in the negative reinforcements. (**a**) Rb1(+) to Rb3(+) control points on beam B1 (C = 20 mm), (**b**) Rb1(+) to Rb3(+) control points on beam B1 (C = 50 mm), (**c**) Rb1(+) to Rb3(+) control points on beam B2 (C = 20 mm), (**d**) Rb1(+) to Rb3(+) control points on beam B2 (C = 50 mm).

The conclusions regarding the efficiency of the concrete mix in the temperature range in the cross-section are similar to the previous ones, with C17-WFC3 being the more interesting solution and C4-RPg being a concrete with a similar performance to the conventional concrete. B1 is more damaged by fire than B2, which is due to the different geometries of the two. In the case of B1, the maximum temperature difference between the two extreme concrete cases (C17-WFC3 and C4-RPg) is 400 °C. If the difference between the reference concrete and C17-WFC3 is considered, these differences are in the order of 500 °C. If B2 is assumed, the difference between the extremes is reduced to 240 °C. If we look at the difference between the reference concrete and C17-WFC3, the differences are in the order of 300 °C.

3.4. Cross-Sectional Temperature Field

The temperature field in the B1 and B2 cross-sections is shown in Figures 6 and 7. This comparison was carried out with beams with the same concrete case (the reference concrete was assumed). The figures illustrate the influence of the geometrical properties of the cross-section on the temperature field and also show that the temperature profile is not uniform, justifying the use of the average temperature as a criterion for the study. This lack of uniformity explains the complexity of fire design and suggests that the average temperature is the more reasonable philosophy to understand the degree of heating in reinforced concrete structures.

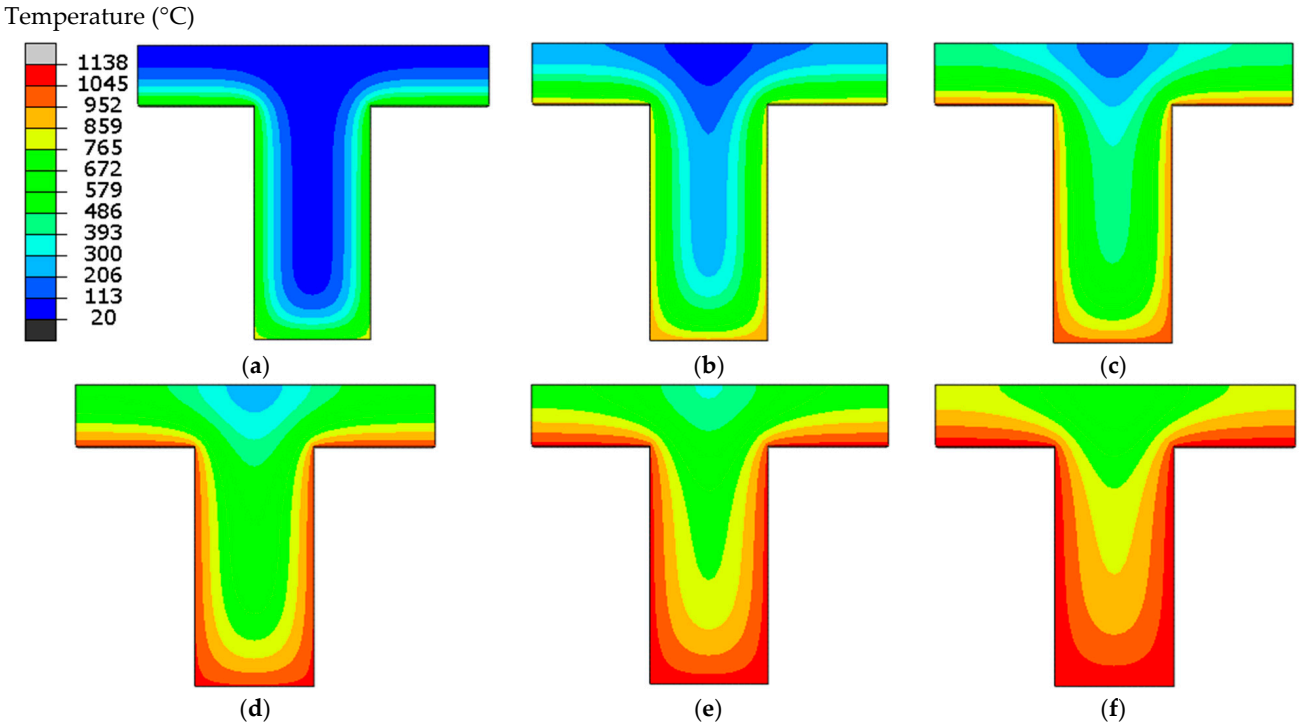


Figure 6. Temperature field in the beam cross-section during different times of the ISO 834 fire (B1 cross-section). (**a**) 30 min, (**b**) 60 min, (**c**) 90 min, (**d**) 120 min, (**e**) 150 min, (**f**) 180 min.

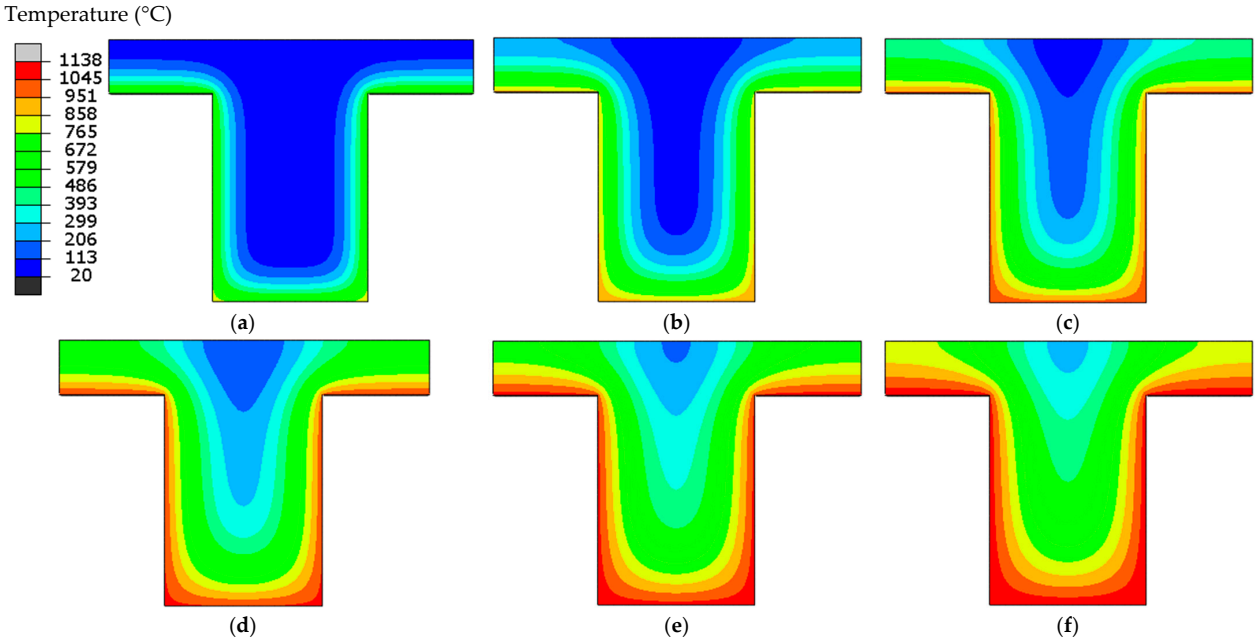


Figure 7. Temperature field in the beam cross-section during different times of the ISO 834 fire (B2 cross-section). (**a**) 30 min, (**b**) 60 min, (**c**) 90 min, (**d**) 120 min, (**e**) 150 min, (**f**) 180 min.

The cross-sectional temperature field highlighted above describes how the temperature is distributed in the cross-section of the structure when it is exposed to fire under the conditions shown in Figure 2.

4. Conclusions

The main conclusions of the proposed research are:

- In the proposed research, the level of fire safety of environmentally friendly concrete was assessed in an unprecedented way, relating aspects of sustainability to building safety;
- The tested green concretes (eco-friendly) showed an interesting potential to provide a good safety performance of structures exposed to fire conditions;
- The temperature fields generated in the green concretes are lower than in conventional concrete in all cases tested, which indicates less mechanical damage to the eco-friendly concretes compared to the conventional solutions;
- In terms of the temperature field in the cross-section of the structure exposed to fire, the beams with a concrete mix of 40% wood and 3% foam produced an average temperature (after 180 min of exposure to fire) that was 50% lower in relation to conventional concrete, making the structure more stable in high temperatures;
- With this eco-friendly concrete, the time in which the reinforcement reaches its critical temperature can be improved by up to 80 min in the event of a fire, which means a 260% improvement in fire resistance rate of the beams tested;
- The concrete with the worst fire performance was the one with a 50% recycled plastic content as a substitute for gravel. At the end of the analysis, the temperature difference between the conventional concrete and this green concrete was no more than 60 °C, indicating a very similar thermal behavior between the two;
- Further efforts are needed for future experimental research: the definition of thermal and physical parameters in different temperature ranges. The already published research defines these parameters as temperature-independent, but it is known that the parameters change with the increase of temperature;
- It is important to emphasize that the proposed research only starts from a thermal analysis, and a thermomechanical analysis is needed as future research to be more conclusive;

- Future research should include a mechanical analysis in the fire behavior study of green structures. However, there is a lack of experimental research that wants to examine the mechanical behavior of these concretes under high temperatures, creating obstacles to developing finite numerical models for predicting the thermomechanical behavior of green structures.

Author Contributions: Conceptualization, F.L.B. and A.S.H.; methodology, F.L.B.; software, F.L.B.; validation, F.L.B. and A.S.H.; formal analysis, A.S.H.; investigation, A.S.H.; data curation, F.L.B.; writing—original draft preparation, F.L.B. and A.S.H.; writing—review and editing, F.L.B.; visualization, F.L.B.; supervision, F.L.B.; project administration, F.L.B. All authors have read and agreed to the published version of the manuscript.

Funding: This research received no external funding.

Institutional Review Board Statement: Not applicable.

Informed Consent Statement: Not applicable.

Data Availability Statement: The data presented in this study are available on request from the corresponding author due to ethical aspects.

Conflicts of Interest: The authors declare no conflicts of interest.

Appendix A

Table A1. Concrete mix assumed to each research.

Nomenclature	Cement (Kg/m^3)	Fine Agregate (Kg/m^3)	Coarse Agregate (Kg/m^3)	Polypropylene Sand (Kg/m^3)	Limestone Powder (Kg/m^3)	OW (Kg/m^3)	Abs (Kg/m^3)	PET (Kg/m^3)	Rubber (Kg/m^3)	Foam (Kg/m^3)	Pine Ash (Kg/m^3)	Leave Ash (Kg/m^3)	Wood Agregate (Kg/m^3)	Bio Agregate (Kg/m^3)	Silica Fume (Kg/m^3)	Fly Ash (Kg/m^3)	Rice Husk Ash (Kg/m^3)	CaCl2 (Kg/m^3)	Palm Oil Fuel Ash (Kg/m^3)	Slag (Kg/m^3)	CaO (Kg/m^3)	Water (Kg/m^3)	Additive (FA) (Kg/m^3)	Additive (SP) (Kg/m^3)	Additive (WR) (Kg/m^3)	Additive (PA) (Kg/m^3)	Viscosity Modifier Agent (Kg/m^3)	w/b
C1-OP	350	698	1081	-	-	78	-	-	-	-	-	-	-	-	-	-	-	-	-	-	-	233.65	-	-	-	-	-	0.66
C2-OPw	350	698	1081	-	-	78	-	-	-	-	-	-	-	-	-	-	-	-	-	-	-	231	-	-	-	-	-	0.66
C3-RPs	427.5	0	1056	-	-	-	265	-	-	-	-	-	-	-	22.5	-	-	-	-	-	-	171	-	-	-	-	-	0.40
C4-RPg	427.5	704	528	-	-	-	199	-	-	-	-	-	-	-	22.5	-	-	-	-	-	-	171	-	-	-	-	-	0.40
C5-Ru	-	990	500	-	-	-	-	0	37	-	-	-	-	-	-	-	-	-	-	585	65	225	-	7.8	-	-	-	0.38
C6-Pet	-	990	500	-	-	-	-	84	0	-	-	-	-	-	-	-	-	-	-	585	65	225	-	7.8	-	-	-	0.38
C7-RH10	418.5	697.4	-	-	-	-	-	-	-	22.8	-	-	-	-	-	-	46.5	-	-	-	-	209.2	46.5	-	-	-	-	0.50
C8-RH40	279	697.4	-	-	-	-	-	-	-	22.8	-	-	-	-	-	-	186	-	-	-	-	209.2	186	-	-	-	-	0.75
C9-PO10	418.5	697.4	-	-	-	-	-	-	-	22.8	-	-	-	-	-	-	-	-	46.5	-	-	209.2	46.5	-	-	-	-	0.50
C10-PO40	279	697.4	-	-	-	-	-	-	-	22.8	-	-	-	-	-	-	-	-	186	-	-	209.2	186	-	-	-	-	0.75
C11-WP8	285	673.4	1080	20.3	95	-	-	-	-	-	-	-	-	-	-	-	-	-	-	-	-	197.5	-	-	-	-	-	0.52
C12-WP40	285	439.2	1080	101.6	95	-	-	-	-	-	-	-	-	-	-	-	-	-	-	-	-	197.5	-	-	-	-	-	0.52
C13-CA	270	1009.1	871.4	-	-	-	-	-	-	-	30	0	-	-	-	-	-	-	-	-	-	162	-	4.5	-	-	-	0.60
C14-LA	270	1009.1	871.4	-	-	-	-	-	-	-	0	30	-	-	-	-	-	-	-	-	-	162	-	5.4	-	-	-	0.60
C15-WFC1	399	798	-	-	-	-	-	-	-	4	-	-	116.4	-	-	-	-	-	-	-	-	153	-	-	4.8	-	-	0.38

Table A1. *Cont.*

Nomenclature	Cement (Kg/m^3)	Fine Agregate (Kg/m^3)	Coarse Agregate (Kg/m^3)	Polypropylene Sand (Kg/m^3)	Limestone Powder (Kg/m^3)	OW (Kg/m^3)	Abs (Kg/m^3)	PET (Kg/m^3)	Rubber (Kg/m^3)	Foam (Kg/m^3)	Pine Ash (Kg/m^3)	Leave Ash (Kg/m^3)	Wood Agregate (Kg/m^3)	Bio Agregate (Kg/m^3)	Silica Fume (Kg/m^3)	Fly Ash (Kg/m^3)	Rice Husk Ash (Kg/m^3)	CaCl2 (Kg/m^3)	Palm Oil Fuel Ash (Kg/m^3)	Slag (Kg/m^3)	CaO (Kg/m^3)	Water (Kg/m^3)	Additive (FA) (Kg/m^3)	Additive (SP) (Kg/m^3)	Additive (WR) (Kg/m^3)	Additive (PA) (Kg/m^3)	Viscosity Modifier Agent (Kg/m^3)	w/b
C16-WFC2	399	798	-	-	-	-	-	-	-	7.9	-	-	116.4	-	-	-	-	-	-	-	-	153	-	-	4.8	-	-	0.38
C17-WFC3	399	798	-	-	-	-	-	-	-	12	-	-	116.4	-	-	-	-	-	-	-	-	153	-	-	4.8	-	-	0.38
C18-BBC	375.82	-	-	-	-	-	-	-	-	-	-	-	-	232	-	250.55	208.79	16.7	-	-	-	401.35	-	-	-	-	-	1.07
C19-WBC	375.82	-	-	-	-	-	-	-	-	-	-	-	-	212	-	250.55	208.79	16.7	-	-	-	398.95	-	-	-	-	-	1.06
C20-RHBC	375.82	-	-	-	-	-	-	-	-	-	-	-	-	160	-	250.55	208.79	16.7	-	-	-	429.75	-	-	-	2.51	1.7	1.14

Appendix B

Table A2. Temperatures in the concrete: average between pt1(+) to pt5(+) control points—B1.

Concrete	Fire Exposure Time (min)					
	30	**60**	**90**	**120**	**150**	**180**
Reference	100.5	256.9	394.6	523.1	635.1	731.5
C1-OP	51.1	132.1	213.8	291.7	365.1	432.4
C2-OPw	47.7	127.2	204.9	282.5	354.2	419.6
C3-RPs	92.0	225.2	347.7	460.9	592.2	651.0
C4-RPg	95.7	233.7	360.5	477.3	581.2	671.0
C5-Ru	70.7	180.8	285.9	384.9	475.9	557.4
C6-Pet	71.9	186.3	295.7	398.4	492.4	577.2
C7-RH10	61.2	150.8	237.3	319.1	395.7	465.2
C8-RH40	62.1	152.9	240.2	322.3	399.6	470.3
C9-PO10	59.0	146.1	230.6	312.0	387.1	454.7
C10-PO40	53.7	134.6	214.8	290.9	364.2	428.8
C11-WP8	85.4	215.5	337.3	450.4	552.0	641.2
C12-WP40	59.2	149.1	239.5	327.1	405.5	479.0
C13-CA	83.9	211.9	332.0	443.9	544.7	632.9
C14-LA	82.7	209.4	328.6	439.6	539.8	627.9
C15-WFC1	41.7	106.9	176.1	242.8	306.3	366.2
C16-WFC2	35.0	87.6	147.0	206.1	262.3	314.6
C17-WFC3	34.9	87.1	146.2	204.9	260.7	312.8
C18-BBC	38.7	97.1	161.5	221.5	280.6	336.3
C19-WBC	37.2	94.3	154.6	214.7	273.6	236.6
C20-RHBC	39.0	98.0	161.8	223.4	282.7	338.8

Table A3. Temperatures in the concrete: average between pt1(+) to pt5(+) control points—B2.

Concrete	Fire Exposure Time (min)					
	30	**60**	**90**	**120**	**150**	**180**
Reference	56.3	148.7	245.1	334.1	420.6	501.7
C1-OP	27.6	66.8	116.7	166.7	215.4	261.0
C2-OPw	26.4	62.9	111.9	160.5	207.9	252.0
C3-RPs	47.9	127.9	208.7	285.8	359.4	428.3
C4-RPg	50.3	133.9	217.9	298.2	374.7	445.7
C5-Ru	36.7	98.4	166.2	230.2	294.4	353.2
C6-Pet	38.7	102.5	173.2	241.3	306.8	368.8
C7-RH10	31.2	77.6	131.8	184.9	236.1	283.8
C8-RH40	31.5	78.8	133.7	187.1	238.8	287.5
C9-PO10	30.2	74.6	127.3	180.0	230.1	276.3
C10-PO40	28.1	67.6	117.7	165.6	213.1	257.9
C11-WP8	44.9	122.1	201.9	278.7	352.2	420.8
C12-WP40	30.2	77.6	134.2	189.9	243.7	294.4
C13-CA	44.1	119.7	198.4	274.0	346.5	413.9

Table A3. *Cont.*

Concrete	Fire Exposure Time (min)					
	30	**60**	**90**	**120**	**150**	**180**
C14-LA	43.4	118.0	195.9	270.9	342.7	409.7
C15-WFC1	24.1	51.8	91.5	133.3	174.7	214.5
C16-WFC2	22.3	42.3	73.9	108.9	144.7	179.0
C17-WFC3	22.3	41.4	72.7	108.1	143.6	177.8
C18-BBC	23.2	46.3	81.9	119.0	157.0	193.8
C19-WBC	23.0	44.3	77.8	114.5	151.4	187.0
C20-RHBC	23.3	46.8	83.0	120.2	158.5	195.5

Table A4. Temperatures in the concrete: average between pt1(−) to pt5(−) control points—B1.

Concrete	Fire Exposure Time (min)					
	30	**60**	**90**	**120**	**150**	**180**
Reference	184.4	443.0	628.4	776.3	885.6	966.9
C1-OP	86.5	240.8	377.0	495.8	599.0	686.5
C2-OPw	79.5	232.1	363.0	482.7	548.9	671.2
C3-RPs	234.9	516.1	694.4	825.6	919.8	989.0
C4-RPg	174.8	406.7	584.9	728.2	838.5	922.3
C5-Ru	126.5	323.8	485.4	621.5	733.3	823.3
C6-Pet	129.0	333.2	499.6	638.5	751.5	842.5
C7-RH10	106.8	271.9	411.6	532.5	636.4	723.3
C8-RH40	108.6	275.3	415.8	536.7	641.1	729.1
C9-PO10	102.3	263.9	401.5	522.8	625.7	711.3
C10-PO40	91.6	244.1	377.1	493.0	596.2	680.7
C11-WP8	155.5	379.7	555.9	699.6	812.0	899.1
C12-WP40	103.3	270.5	416.9	545.5	650.5	740.7
C13-CA	152.6	374.2	549.3	692.4	805.1	892.2
C14-LA	150.2	370.2	544.6	687.4	800.2	887.9
C15-WFC1	66.5	194.9	315.8	422.9	518.3	602.3
C16-WFC2	52.2	158.6	266.7	265.9	454.3	532.1
C17-WFC3	52.1	157.8	265.3	363.9	452.0	529.4
C18-BBC	60.2	176.5	291.3	389.9	481.0	561.9
C19-WBC	56.9	171.5	279.6	379.2	470.8	548.5
C20-RHBC	60.9	178.2	291.7	392.7	484.1	565.2

Table A5. Temperatures in the concrete: average between pt1(−) to pt5(−) control points—B2.

Concrete	Fire Exposure Time (min)					
	30	**60**	**90**	**120**	**150**	**180**
Reference	119.8	308.7	468.4	595.3	701.6	788.7
C1-OP	46.5	146.8	251.0	344.6	428.5	501.4
C2-OPw	42.8	137.9	241.8	333.8	416.4	488.0
C3-RPs	100.2	269.8	411.0	530.3	630.9	714.7

Table A5. *Cont.*

Concrete	Fire Exposure Time (min)					
	30	**60**	**90**	**120**	**150**	**180**
C4-RPg	105.9	281.3	425.8	547.6	649.5	733.4
C5-Ru	71.9	213.4	341.3	449.3	547.2	628.3
C6-Pet	77.1	221.5	353.4	466.7	564.3	647.7
C7-RH10	57.3	169.9	278.6	374.7	459.9	533.6
C8-RH40	58.3	172.6	282.0	378.2	464.0	538.7
C9-PO10	54.6	163.6	270.2	366.5	450.7	522.8
C10-PO40	48.5	148.3	252.4	341.7	423.7	495.8
C11-WP8	92.8	259.6	401.3	521.5	622.9	707.5
C12-WP40	54.3	170.3	284.0	384.3	472.9	550.0
C13-CA	90.7	255.0	395.6	514.9	616.0	700.0
C14-LA	89.0	251.8	391.6	510.5	611.2	695.3
C15-WFC1	35.8	112.0	200.9	284.0	360.0	428.5
C16-WFC2	29.5	88.2	163.6	237.5	306.9	369.4
C17-WFC3	29.5	86.0	161.2	235.9	305.0	367.1
C18-BBC	32.8	98.6	179.7	256.9	328.9	394.3
C19-WBC	32.2	93.4	172.0	248.2	318.9	383.0
C20-RHBC	33.1	99.8	183.0	259.2	331.5	397.0

Table A6. Temperatures in the reinforcements: average between Rb1(+) to Rb3(+) control points (C = 50 mm)—B1.

Concrete	Fire Exposure Time (min)					
	30	**60**	**90**	**120**	**150**	**180**
Reference	264.3	571.3	749.8	880.2	968.9	1032.6
C1-OP	128.1	345.4	513.6	645.5	749.8	831.4
C2-OPw	117.4	334.2	497.8	632.5	737.0	818.6
C3-RPs	243.3	522.6	701.0	831.7	925.0	993.4
C4-RPg	252.7	536.3	715.3	845.6	937.5	1004.0
C5-Ru	186.2	445.9	625.3	760.0	860.4	935.9
C6-Pet	189.4	456.4	638.3	773.9	874.0	949.5
C7-RH10	158.6	385.2	552.1	681.7	783.1	861.8
C8-RH40	161.2	389.4	556.5	685.7	787.1	866.3
C9-PO10	152.0	375.2	541.1	672.6	774.0	852.1
C10-PO40	136.0	350.2	514.4	643.4	748.0	827.3
C11-WP8	226.2	507.4	689.7	823.2	918.5	988.3
C12-WP40	152.9	382.6	556.5	693.1	794.1	874.6
C13-CA	222.3	501.5	683.8	817.6	913.6	983.7
C14-LA	218.9	497.2	679.6	813.6	910.0	980.7
C15-WFC1	97.6	285.4	443.1	570.4	674.4	759.2
C16-WFC2	75.0	235.3	382.4	506.6	609.1	692.9
C17-WFC3	74.9	234.2	380.7	504.5	606.7	690.4

Table A6. *Cont.*

Concrete	Fire Exposure Time (min)					
	30	**60**	**90**	**120**	**150**	**180**
C18-BBC	87.8	260.3	413.4	534.2	637.2	721.9
C19-WBC	82.5	253.3	398.7	521.9	626.7	709.0
C20-RHBC	88.9	262.7	413.9	537.3	640.3	725.0

Table A7. Temperatures in the reinforcements: average between Rb1(+) to Rb3(+) control points (C = 50 mm)—B2.

Concrete	Fire Exposure Time (min)					
	30	**60**	**90**	**120**	**150**	**180**
Reference	262.5	525.1	689.8	806.7	892.2	957.6
C1-OP	127.3	335.0	487.2	603.7	694.9	766.5
C2-OPw	116.9	320.8	476.3	592.6	684.0	755.4
C3-RPs	237.2	490.5	646.7	763.6	849.5	915.5
C4-RPg	84.2	203.6	311.5	408.7	494.5	569.3
C5-Ru	183.2	423.9	582.0	698.4	790.1	859.1
C6-Pet	192.7	432.6	592.7	712.4	801.9	871.7
C7-RH10	157.4	371.7	521.4	635.4	724.2	793.5
C8-RH40	159.8	375.6	525.1	638.8	727.6	797.5
C9-PO10	150.9	362.8	511.9	627.7	716.5	785.2
C10-PO40	135.4	339.9	491.5	602.7	692.5	763.6
C11-WP8	220.7	476.4	636.2	755.3	842.8	909.9
C12-WP40	146.0	368.4	523.9	641.7	732.6	803.9
C13-CA	217.0	471.3	631.0	750.3	838.1	905.2
C14-LA	213.9	467.6	627.5	746.8	834.8	902.2
C15-WFC1	97.4	279.7	425.7	539.6	631.2	705.1
C16-WFC2	74.9	235.6	373.2	484.0	575.3	648.7
C17-WFC3	74.8	231.1	369.4	482.2	573.2	646.5
C18-BBC	87.6	256.0	396.9	508.2	599.5	673.5
C19-WBC	85.7	245.9	385.9	497.6	588.7	662.5
C20-RHBC	88.7	258.3	401.9	511.0	602.2	676.3

Table A8. Temperatures in the reinforcements: average between Rb1(−) to Rb3(−) control points (C=50 mm)—B1.

Concrete	Fire Exposure Time (min)					
	30	**60**	**90**	**120**	**150**	**180**
Reference	40.0	124.0	231.5	349.5	465.6	573.6
C1-OP	23.7	48.0	87.4	134.9	187.6	241.9
C2-OPw	23.0	45.9	82.2	128.4	178.7	230.5
C3-RPs	35.4	99.4	186.0	281.8	379.5	472.9
C4-RPg	37.0	105.6	197.8	298.9	401.2	497.3
C5-Ru	28.6	72.5	136.6	210.6	289.4	367.1

Table A8. *Cont.*

Concrete	Fire Exposure Time (min)					
	30	**60**	**90**	**120**	**150**	**180**
C6-Pet	29.1	75.9	144.4	223.2	306.5	389.6
C7-RH10	25.7	56.1	101.5	154.7	212.7	198.2
C8-RH40	25.9	57.1	103.3	157.1	216.1	201.4
C9-PO10	25.2	53.9	97.3	149.3	205.3	191.6
C10-PO40	24.1	48.9	87.6	133.8	186.0	237.9
C11-WP8	33.6	94.0	178.3	272.7	369.7	462.7
C12-WP40	25.4	55.8	103.6	161.7	222.4	286.2
C13-CA	33.0	91.7	173.9	266.4	361.7	453.1
C14-LA	32.6	90.1	171.0	262.1	356.3	447.1
C15-WFC1	22.0	38.1	66.5	101.8	141.7	184.6
C16-WFC2	21.1	31.8	52.6	80.2	111.6	145.1
C17-WFC3	21.1	31.7	52.3	79.6	110.6	143.8
C18-BBC	21.6	34.7	59.2	88.9	123.6	161.2
C19-WBC	21.4	33.8	56.0	85.0	118.9	153.8
C20-RHBC	21.7	35.0	59.4	89.9	125.1	163.0

Table A9. Temperatures in the reinforcements: average between Rb1(−) to Rb3(−) control points (C = 50 mm)—B2.

Concrete	Fire Exposure Time (min)					
	30	**60**	**90**	**120**	**150**	**180**
Reference	38.6	99.0	177.3	258.3	342.3	424.3
C1-OP	23.5	45.0	76.0	110.8	147.9	185.5
C2-OPw	22.9	42.7	72.8	106.2	141.8	177.6
C3-RPs	33.9	83.8	145.0	211.4	279.9	347.0
C4-RPg	35.2	88.1	152.9	223.1	295.2	365.3
C5-Ru	28.0	64.0	110.9	161.5	217.1	271.6
C6-Pet	29.0	66.5	116.3	171.5	228.9	287.0
C7-RH10	25.4	51.7	86.6	124.8	165.3	205.9
C8-RH40	25.6	52.5	87.9	126.6	167.6	209.2
C9-PO10	25.0	49.9	83.5	121.1	160.2	199.2
C10-PO40	23.9	45.8	77.1	110.3	146.3	182.9
C11-WP8	32.3	79.7	139.5	204.9	272.8	339.7
C12-WP40	24.8	51.2	87.8	128.4	171.6	215.6
C13-CA	31.9	78.0	136.5	200.6	267.2	332.7
C14-LA	31.5	76.8	134.5	197.7	263.5	328.3
C15-WFC1	21.9	36.7	60.2	87.2	116.3	146.5
C16-WFC2	21.1	31.5	49.5	71.2	94.8	119.1
C17-WFC3	21.1	31.0	48.9	70.7	94.1	118.2
C18-BBC	21.5	33.7	54.1	77.8	103.5	130.3
C19-WBC	21.4	32.6	51.9	74.8	99.6	125.2
C20-RHBC	21.6	34.0	55.0	78.6	104.6	131.6

References

1. Andrew, R.M. Global CO_2 emissions from cement production. *Earth Syst. Sci. Data* **2018**, *10*, 195–217. [CrossRef]
2. Boukhari, M.E.L.; Merroun, O.; Maalouf, C.; Bogard, F.; Kissi, B. Exploring the impact of partial sand replacement with olive waste on mechanical and thermal properties of sustainable concrete. *Clean. Mater.* **2023**, *9*, 100202. [CrossRef]
3. El-Aidy, K.E.; Ellithy, M.; Mahmoud, M.H.; El-Shafiey, T.F. Mechanical and physical properties of eco-friendly recycled plastic concrete (RPC). *J. Build. Eng.* **2024**, *97*, 110907. [CrossRef]
4. Aghamohammadi, O.; Jafari, Z.; Bahmani, H.; Mostofinejad, D. Novel eco-friendly high-strength concrete based on slag activated with calcium oxide: Environmental, thermal and mechanical performance. *Constr. Build. Mater.* **2024**, *449*, 138334. [CrossRef]
5. Tamburini, E.; Krozer, Y.; Castaldelli, G. How much are we paying for drinking water in (PET) bottles? A global assessment of the hidden costs and potential damage to the environment. *Environ. Chall.* **2025**, *18*, 101083. [CrossRef]
6. Mydin, M.A.O.; Sor, N.H.; Althoey, F.; Özkılıç, Y.O.; Al Bakri Abdullah, M.M.; Isleem, H.F.; Deifalla, A.F.; Tawfik, T.A. Performance of lightweight foamed concrete partially replacing cement with industrial and agricultural wastes: Microstructure characteristics, thermal conductivity and hardened properties. *Ain Shams Eng. J.* **2023**, *14*, 102546. [CrossRef]
7. Ahmed, S.N.; Sor, N.H.; Ahmed, M.A.; Qaidi, S.M.A. Thermal conductivity and hardened behavior of eco-friendly concrete incorporating waste polypropylene as fine aggregate. *Mater. Today Proc.* **2022**, *57*, 818–823. [CrossRef]
8. Gharibi, H.; Mostofinejad, D.; Teymouri, M. Impacts of Conifer Leaves and Pine Ashes on Concrete Thermal Properties. *Constr. Build. Mater.* **2023**, *377*, 131144. [CrossRef]
9. Xu, C.; Li, Q.; Wang, P.; Guo, Y. Preparation and performance research of ecological concrete using waste wood. *Case Stud. Constr. Mater.* **2024**, *20*, e03221. [CrossRef]
10. de Lima Moura Paiva, R.; Santos, D.O.J.D.; de Aguiar, A.L.D.; da Cunha Gomes, B.M.; Bezerra, C.G.; Hasparyk, N.P.; Filho, R.D.T. Influence of bio-aggregates on the physical and hygrothermal properties of bio-concretes. *Constr. Build. Mater.* **2024**, *456*, 139218. [CrossRef]
11. *EN 1992-1.1*; Eurocode 2: Design of Concrete Structures—Part 1-1: General Rules and Rules for Buildings. European Committee for Standardization: Brussels, Belgium, 2004.
12. Abaqus. *Abaqus Analysis User's Guide*; Simulia: Johnston, RI, USA, 2016.
13. *EN 1992-1.2*; Eurocode 2: Design of Concrete Structures—Part 1-2: General Rules—Structural Fire Design. European Committee for Standardization: Brussels, Belgium, 2004.
14. Bolina, F.; Tutikian, B.; Rodrigues, J.P.C. Thermal analysis of steel decking concrete slabs in case of fire. *Fire Saf. J.* **2021**, *121*, 103295. [CrossRef]
15. Bolina, F.L.; Schallenberger, M.; Carvalho, H. Experimental and numerical evaluation of RC ribbed slabs in fire conditions. *Structures* **2023**, *51*, 747–759. [CrossRef]
16. Banerji, S.; Kodur, V. Numerical model for tracing the response of Ultra-High performance concrete beams exposed to fire. *Fire Mater.* **2023**, *47*, 322–340. [CrossRef]
17. *ISO 834*; Fire-Resistance Tests—Elements of Building Construction—Part 1: General Requirements. ISO: Geneva, Switzerland, 1999.
18. Bolina, F.L.; Poleto, G.; Carvalho, H. Proposition of parametric data for UHPC at high temperatures. *J. Build. Eng.* **2023**, *76*, 107222. [CrossRef]
19. Bolina, F.L.; Rodrigues, J.P.C. Finite element analysis criteria for composite steel decking concrete slabs subjected to fire. *Fire Saf. J.* **2023**, *139*, 103818. [CrossRef]
20. Kodur, V.K.R.; Phan, L. Critical factors governing the fire performance of high strength concrete systems. *Fire Saf. J.* **2007**, *42*, 482–488. [CrossRef]
21. *FIB Bulletin 38*; Fire Design of Concrete Structures—Materials, Structures and Modelling—State of Art Report. Fédération Internationale du Béton: Lausanne, Switzerland, 2007.
22. Handousa, A.M.; Abdellatief, M.; Salem, F.A.; Mahmoud, N.; Ghannam, M. Experimental and analytical study on axial behaviour of square corrugated concrete filled single and double skin tube stub columns. *Sci. Rep.* **2025**, *15*, 2167. [CrossRef] [PubMed]

Disclaimer/Publisher's Note: The statements, opinions and data contained in all publications are solely those of the individual author(s) and contributor(s) and not of MDPI and/or the editor(s). MDPI and/or the editor(s) disclaim responsibility for any injury to people or property resulting from any ideas, methods, instructions or products referred to in the content.